11-25-1999

# Recent laboratory tests of a hard x-ray solar flare polarimeter

Mark L. McConnell
*University of New Hampshire - Main Campus*, mark.mcconnell@unh.edu

John R. Macri
*University of New Hampshire - Main Campus*, John.Macri@unh.edu

M McClish
*University of New Hampshire - Main Campus*

Jack Ryalls
*University of Central Florida*

### Recommended Citation

Mark L. McConnell ; John R. Macri ; Mickel McClish and James M. Ryan "Recent laboratory tests of a hard x-ray solar flare polarimeter", Proc. SPIE 3764, Ultraviolet and X-Ray Detection, Spectroscopy, and Polarimetry III, 70 (November 25, 1999); doi:10.1117/12.371100; http://dx.doi.org/10.1117/12.371100

# Recent Laboratory Tests of a Hard X-Ray Solar Flare Polarimeter

M.L. McConnell*, J.R. Macri, M. McClish and J. Ryan

Space Science Center, Morse Hall, University of New Hampshire, Durham, New Hampshire 03824

## ABSTRACT

We report on the development of a Compton scatter polarimeter for measuring the linear polarization of hard X-rays (50-300 keV) from solar flares. Such measurements would be useful for studying the directivity (or beaming) of the electrons that are accelerated in solar flares. We initially used a simple prototype polarimeter to successfully demonstrate the reliability of our Monte Carlo simulation code and to demonstrate our ability to generate a polarized photon source in the lab. We have recently fabricated a science model based on a modular design concept that places a self-contained polarimeter module on the front-end of a 5-inch position-sensitive PMT (PSPMT). The PSPMT is used to determine the Compton interaction location within an annular array of small plastic scintillator elements. Some of the photons that scatter within the plastic scintillator array are subsequently absorbed by a small centrally-located array of CsI(Tl) crystals that is read out by an independent multi-anode PMT. The independence of the two PMT readout schemes provides appropriate timing information for event triggering. We are currently testing this new polarimeter design in the laboratory to evaluate the performance characteristics of this design. Here we present the initial results from these laboratory tests. The modular nature of this design lends itself toward its accomodation on a balloon or spacecraft platform. A small array of such modules can provide a minimum detectable polarization (MDP) of less than 1% in the integrated 50-300 keV energy range for X-class solar flares.

Keywords: Hard X-Rays, Polarimetry, Solar Flares, Gamma-Ray Bursts, PSPMT

## 1. INTRODUCTION

The basic physical process used to measure linear polarization of hard X-rays (50–300 keV) is Compton scattering.[1] In general, the scattering geometry can be described by two angles. The first of these is the *Compton scatter angle* ($\theta$), the angle between the incident and scattered photons. A second angle ($\eta$) defines the scattered photon direction as projected onto a plane perpendicular to the incident photon direction. This angle, which we refer to as the *azimuthal scatter angle*, is measured from the plane containing the electric vector of the incident photon. For a given value of $\theta$, the scattering cross section for polarized radiation reaches a minimum at $\eta = 0°$ and a maximum at $\eta = 90°$. In other words, photons tend to be Compton scattered at right angles relative to the plane of polarization of the incident radiation. In the case of a Compton scatter polarimeter, this asymmetry, which is maximized for values of $\theta$ near 90°, is exploited as a means to determine the linear polarization parameters of the incident radiation. The successful design of a polarimeter hinges on the ability to reconstruct the kinematics of each event. In this context, we can consider: 1) the ability to measure the energies of both the scattered photon and the scattered electron; and 2) the ability to measure the scattering geometry.

A Compton scatter polarimeter consists of two detectors that are used to measure the energies of both the scattered photon and the scattered electron.[2, 3] These measurements also serve to define the scattering geometry. One detector (the *scattering detector*) provides the medium for the Compton interaction to take place. This detector must be designed to maximize the probability of a single Compton interaction with a subsequent escape of the scattered photon. This implies a low-Z material that is sufficiently thick to induce a single Compton scattering, but thin enough to minimize the chance of subsequent interactions. The second detector (the *calorimeter*) absorbs the remaining energy of the scattered photon. Information regarding the scattering geometry comes from the relative location of the detectors. Knowledge of the scattering geometry can be further improved by measuring the interaction location *within* each detector. The accuracy with which the scattering geometry can be measured determines the ability to define the modulation pattern and therefore has a direct impact on the polarization sensitivity.

---

* Correspondence: E-mail: Mark.McConnell@unh.edu

With regard to the definition of the modulation pattern (which follows a $\cos 2\eta$ distribution), it is customary to define, as a figure-of-merit for the polarimeter, the *polarization modulation factor*.[2] For a given energy and incidence angle of an incoming photon beam, this can be expressed as,

$$\mu_P = \frac{C_{max}(P) - C_{min}(P)}{C_{max}(P) + C_{min}(P)} \tag{1}$$

where $C_{max}$ and $C_{min}$ are the maximum and minimum number of counts registered in the polarimeter, respectively, with respect to the azimuthal scatter angle ($\eta$). It is useful to define the modulation factor which results from an incident beam that is 100% polarized,

$$\mu_{100} = \frac{C_{max}(100\%) - C_{min}(100\%)}{C_{max}(100\%) + C_{min}(100\%)} \tag{2}$$

We then use this result (often derived from Monte Carlo simulations), together with the observed modulation factor ($\mu_P$), to determine the level of polarization in a measured beam,

$$P = \frac{\mu_P}{\mu_{100}} = \frac{1}{\mu_{100}} \frac{C_{max}(P) - C_{min}(P)}{C_{max}(P) + C_{min}(P)} \tag{3}$$

The $3\sigma$ sensitivity for measuring polarization is then,[2]

$$P(3\sigma) = \frac{3}{\mu_{100} S} \left[ \frac{2(S + B)}{T} \right]^{1/2} \tag{4}$$

where $S$ is the source count rate, $B$ is the background count rate, $\mu_{100}$ is the modulation factor for 100% polarization and $T$ is the observation time. We see that improved sensitivity to source polarization can be achieved either by increasing the modulation factor ($\mu_{100}$) or by increasing the effective area of the polarimeter (thereby increasing the source count rate).
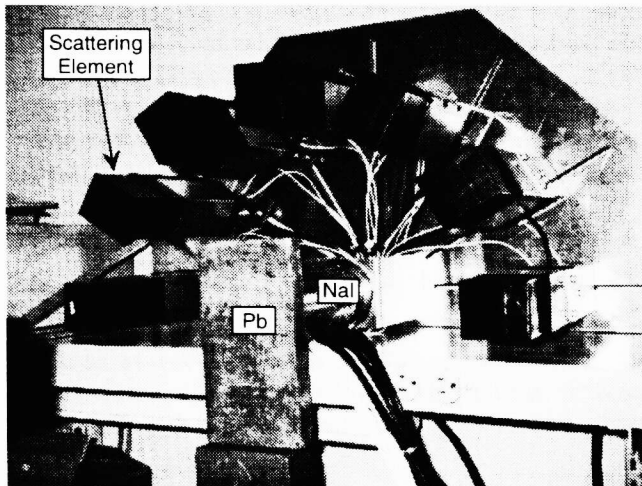
## 2. LABORATORY PROTOTYPE



Figure 1: The laboratory prototype showing the plastic scattering elements surrounding the central NaI detector. A lead block was used to shield the NaI detector from direct flux.

In our earliest work, we discussed a simple polarimeter design consisting of a ring of twelve individual scattering detectors (composed of low-Z plastic scintillator) surrounding a single NaI calorimeter.[4] To be recorded as a polarimeter event, an incident photon Compton scatters from one (and only one) of the scattering detectors into the central calorimeter. The incident photon energy can be determined from the sum of the energy losses in both detectors. The azimuthal scattering angle ($\eta$) can be determined by the azimuthal angle of the associated scattering detector. When the polarimeter is arranged so that the incident flux is parallel to the symmetry axis, unpolarized radiation will produce an axially symmetric coincidence rate. If, on the other hand, the incident radiation is linearly polarized, then the coincidence rate will show an azimuthal asymmetry whose phase depends on the position angle of the incident radiation's electric field vector and whose magnitude depends on the degree of polarization. The characteristics of this design were investigated using a series of Monte Carlo simulations that were based on a modified version of the GEANT simulation package.
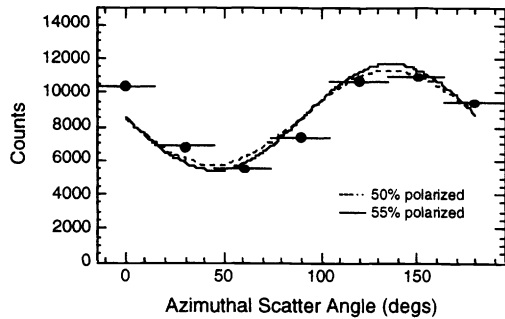
71

Figure 3: The prototype response to a polarized beam incident on-axis, but with a polarization angle rotated ~45° with respect to that in Figure 4. The smooth curves represent simulation results.
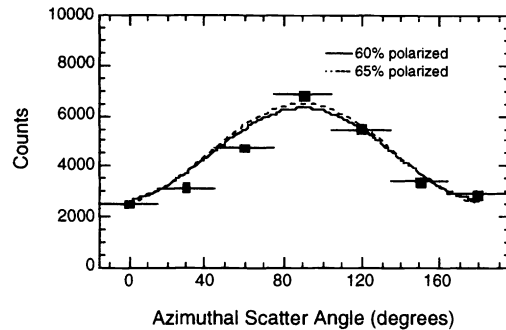


Figure 2: The prototype response to a polarized beam incident on-axis. The smooth curves represent simulation results.

A prototype of this design was tested in the laboratory, in part to validate our Monte Carlo code.[5, 6] For testing purposes, we set up a semicircular array of plastic scintillator elements around a central NaI detector. This semicircular design retained the fundamental physics, but, by eliminating the redundancy, simplified the hardware and associated electronics. A photograph of the laboratory setup is shown in Figure 1. A source of polarized photons was generated by Compton scattering photons from a radioactive source.[7] The exact level of polarization of such a scattered photon beam is dependent on both the initial photon energy and the photon scatter angle.[6, 8] The use of plastic scintillator as a scattering block in generating the polarized beam permits the electronic tagging of the scattered (polarized) photons. This is especially useful in identifying (via coincidence techniques) the interaction of the polarized photons in the polarimeter.

Results from the prototype testing are shown in Figures 2 and 3, where we show the measured data along with Monte Carlo simulation results for two different polarization angles. The polarization values derived from these data agree well with that expected from the laboratory polarization geometry. These results demonstrated: a) the ability of a simple Compton scatter polarimeter to measure hard X-ray polarization; b) the ability of our Monte Carlo code to predict the polarimeter response; and c) the ability to generate a source of polarized photons using a simple scattering technique.

## 3. DESIGNING A HARD X-RAY POLARIMETER

The goal of our program has been to develop a hard X-ray polarimeter that would be suitable for studying solar flare emissions. Such a polarimeter must meet the following requirements: 1) it must be compact and light-weight in order to conform with various budget restrictions imposed on any realistic payload; 2) it must be modular in order to provide flexibility as a piggy-back payload and to permit building up an array of detectors with sufficient sensitivity; 3) it must have reasonable detection efficiency over a broad energy range (50–300 keV); and 4) it must have polarization sensitivity below 10% in the 50–300 keV energy range for a moderately-sized (class M5) solar flare. (Based on SMM-GRS observations during the 1980–82 solar maximum, we can expect >50 flares of class M5 or larger during the upcoming solar maximum period.)

### 3.1. Design considerations

There are at least two possible means of optimizing the performance of a Compton scatter polarimeter: 1) by more precisely measuring the scattering geometry of each event; and 2) by rejecting those events that undergo multiple Compton scattering within the scattering elements. A better geometry definition will serve to more clearly define the modulation pattern of the incident flux. Improved rejection of multiple scatter events will reduce the contribution of such events to the unmodulated component of the polarization response.

An improvement in the measured scattering geometry of an event can be achieved by improving the spatial resolution within each detector element. Fully 3-dimensional spatial information is generally not crucial. Since we are principally interested in the azimuthal scattering angle ($\mu$) of each event, spatial information in the x–y plane (i.e., parallel to the front surface of the

polarimeter) will be of greatest importance. Although dependent on the precise geometry of the polarimeter, additional information regarding the z–component of the location will generally add little to the information content of the event.

At these energies (50–300 keV), multiple scatter events in the central calorimeter can be safely ignored due to the dominance of the photoelectric effect (assuming that the calorimeter consists of some high-Z inorganic scintillator such as NaI or CsI). Multiple scatter events can be important when the pathlength through the scattering elements becomes comparable to the mean free path of the incident photons (about 6 cm at 100 keV). Since the detection efficiency is, to a great extent, proportional to volume, the geometry of the scattering elements (in terms of both surface area and depth) must be carefully chosen so as to reach a compromise between detection efficiency and the generation of multiple scatter events. If, on the other hand, one can acquire information about the spatial *distribution* of energy deposits, it then becomes possible to distinguish those events with more than one interaction site (i.e., multiple scatter events). Such events can subsequently be rejected during the analysis. This capability would permit the effective use of larger volumes of plastic scintillator, with the potential for a subsequent increase in polarimeter sensitivity. Given the relatively large mean free path of the photons at these energies, a spatial resolution of ~1.0 cm is sufficient to reject a large fraction of the multiple scatter events. Smaller spatial resolutions may be desirable for improving the definition of the scatter geometry.
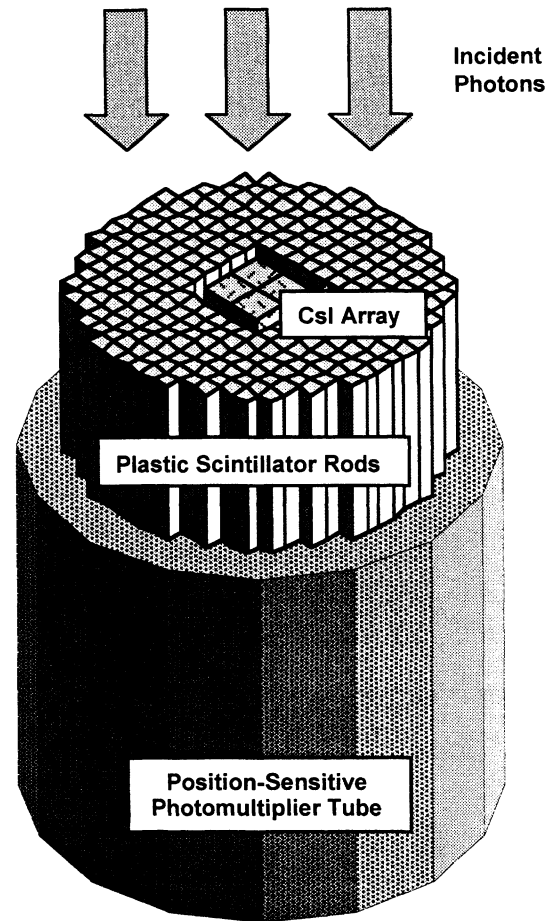


Figure 4: The SOLPOL polarimeter design showing the layout of the plastic scintillator elements and CsI(Tl) elements on the front surface of a PSPMT. Not shown here is the 4-element multianode PMT used for readout of the CsI(Tl) array and the lead shield that would be used to block direct flux from the CsI(Tl) array.

Two other practical considerations should be noted. In order to reduce accidental coincidences that may be associated with high incident flux levels (such as that from a solar flare), there is a need to shield the calorimeter detectors from direct flux. A thin layer of lead (5 mm thick) is sufficient for this purpose. A second consideration is that of systematic variations in the azimuthal scatter angle distribution due, for example, to detection nonuniformities in the scattering elements. One way to ameliorate this condition is by continuously rotating the polarimeter about its axis of symmetry.

## 3.2. A Modular Polarimeter Design

Based, in part, on the above considerations, we have developed a modular polarimeter design that places an entire device on the front end of a single 5-inch diameter position-sensitive PMT (PSPMT).[6,9] Since the focus of our efforts has so far been directed toward solar studies, we refer to this new design as SOLPOL (for SOLar POLarimeter). The design incorporates an array of plastic scintillator elements to provide the improved spatial resolution in the scattering medium and to improve the rejection of multiple scatter events. Each plastic scintillator element is optically-isolated with a cross sectional area of 5 × 5 mm². The plastic elements are arranged in the form of an annulus having an outside diameter of 10 cm (corresponding to the sensitive area of the Hammatsu R3292 5-inch PSPMT). The central portion of the annulus is large enough to insert a small 2 × 2 array of 1 cm CsI(Tl) scintillators. The CsI(Tl) scintillators are coupled to their own independent multi-anode PMT (MAPMT) for the energy measurement and signal timing. In the baseline design, depicted in Figure 4, both the plastic and CsI(Tl) elements have a depth of 5 cm. An ideal SOLPOL event is one in which the incident photon Compton scatters in one plastic element, with the remaining photon energy subsequently absorbed in the central CsI array.
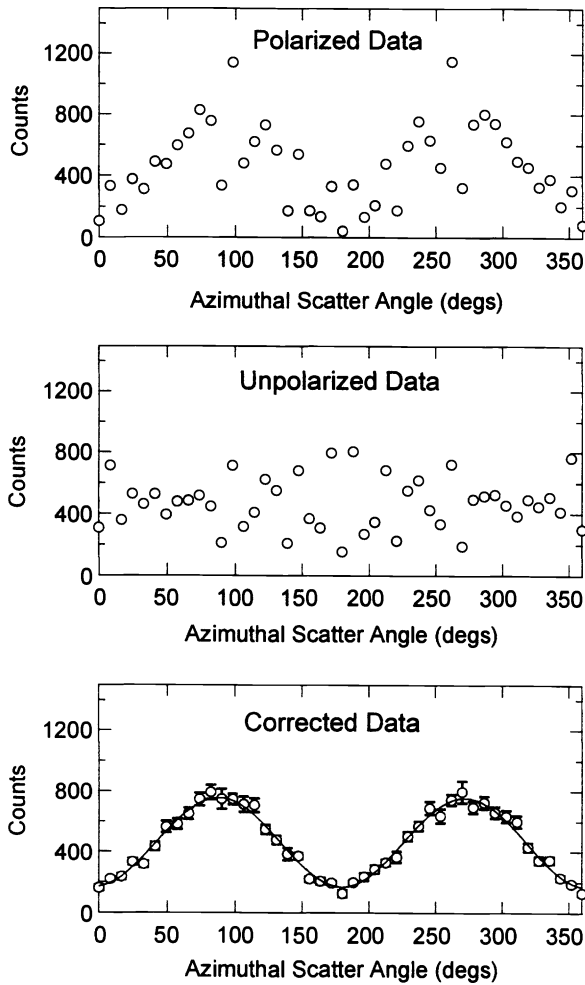
73

Figure 5: Simulated polarimeter data showing how the measured data is corrected for intrinsic geometric effects to extract the true modulation pattern. These data correspond to the response of the baseline SOLPOL design to a monoenergetic beam of 150 keV photons incident at 0°.
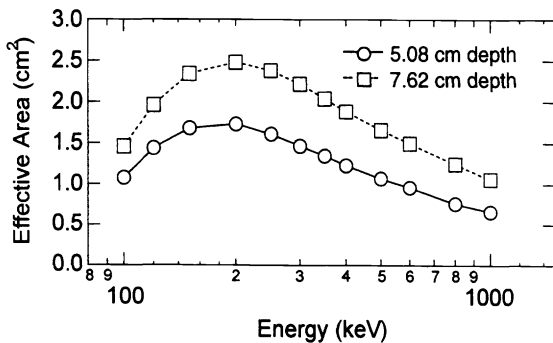
We have completed a series of Monte Carlo simulations to determine the charcteristics of this design. These simulations assume that we are able to uniquely identify which plastic scintillator element is involved in the event. The small cross-sectional area of each scintillator element ensures that practically all multiple scatter events are rejected. The energy threshold levels, particularly in the scattering elements, have a significant influence on the performance of the polarimeter at low energies. For the simulations, we have assumed a threshold energy of 15 keV in both the plastic and CsI scintillators.

Figure 5 illustrates the nature of the SOLPOL data. In this case, the data are from Monte Carlo simulations using the baseline SOLPOL design (Figure 4). The first panel shows the polarization response to a fully polarized monoenergetic beam of 150 keV photons vertically incident on the front surface of the polarimeter. This distribution includes not only the intrinsic modulation pattern due to the Compton scattering process, but it also includes geometric effects related to the specific layout of the detector elements within the polarimeter and the associated quantization of possible scatter angles. The geometric effects can be more clearly seen in the case of an incident beam that is completely unpolarized, as shown in the second panel of Figure 5. (In practice, for analyzing real data, this unpolarized distribution would be determined by simulations rather than by direct measurements.) To extract the true distribution of polarized events, we divide the polarized distribution by the unpolarized distribution and normalize by the average of the unpolarized distribution. Only when we correct the raw data in this fashion do we clearly see the cos 2η modulation pattern that is expected (the third panel of Figure 5).

Simulated data have also been used to evaluate the performance characteristics of the baseline design. Figures 6 and 7 show the effective area and modulation factor, respectively, as a function of incident photon energy. In



Figure 6: The effective area as a function of energy for the baseline design having a depth of both 5.08 cm and 7.62 cm.
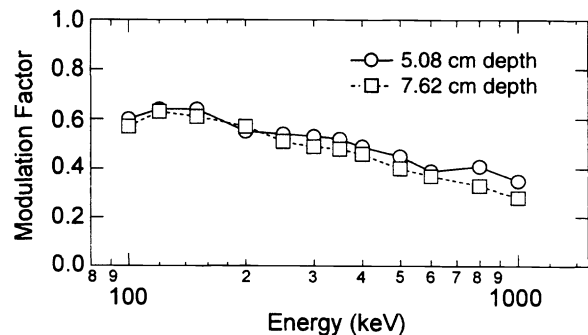


Figure 7: The modulation factor as a function of energy for the baseline design having depths of 5.08 cm and 7.62 cm.
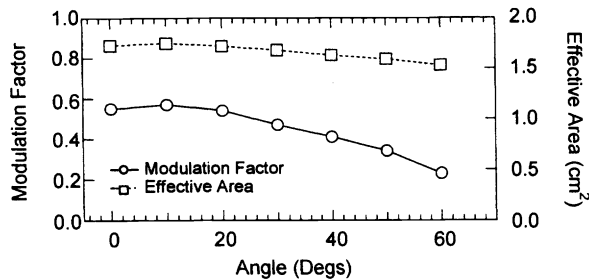
Figure 8: The modulation factor and effective area at 200 keV for various incidence angles. The polarimeter maintains good response out to 60° incidence angles.

both cases, are shown the results for two different detector depths – 5.08 cm (as depicted in Figure 4) and 7.62 cm. Although the deeper detector clearly presents an advantage in terms of effective area, the varying detector depth appears to have little influence on the modulation factor. In practice, the advantage of increased effective area for a deeper detector must be offset by the increase in background as well as the decrease in light collection efficiency (with its consequent effects on the detector threshold).

One potentially useful aspect of the SOLPOL design is that there exists a significant polarization response at large off-axis angles. This can be seen in Figure 8, which is based on simulations with a detector depth of 5.08 cm. The effective area remains relatively constant at large angles. This results from the fact that the exposed geometric area of the detector remains relatively constant. Although there is a significant decrease in the modulation factor at large angles, there is still significant polarization response even at 60° incidence angle. The off-axis response of this design would be very useful, for example, in studies of gamma-ray bursts.

## 4. SCIENCE MODEL FABRICATION AND TESTING

We have recently completed the fabrication of a science model based on the modular SOLPOL design. The plastic scintillator array is composed of individual pieces of Bicron BC-404 scintillator. Each 5 mm × 5 mm × 50 mm scintillator element is individually wrapped in Tyvek® to maximize light collection efficiency and to provide optical isolation. A thin layer of Kapton® tape was then used to hold the wrapping in place. A thin aluminum housing encloses both the PSPMT and the plastic scintillator array. The calorimeter detector assembly is a 2 × 2 array of 1 cm CsI(Tl) elements coupled to a MAPMT (Hamamatsu R5900 with a 2 × 2 anode array) and enclosed within its own, separate light-tight housing. During operations, the calorimeter detector assembly is inserted into a central well in the PSPMT / plastic scintillator housing. Data processing and acquisition is achieved using a combination of NIM and CAMAC modules, with the final data recorded via a SCSI interface on a Macintosh computer.

The initial laboratory tests make use of a charge division network for the PSPMT (Hammamatsu R3292) that provides a weighted average of the spatial distribution of the measured light output using only four signals (two signals in x and 2 signals in y). In principle, more precise information regarding the distribution of energy deposits within the plastic arrays can be derive from using all 56 (28-x plus 28-y) anode signals from the PSPMT. We first plan to pursue an intermediate approach using only fourteen (7-x plus 7-y) anode wire sections. Such



Figure 9: Distribution of measured polarimeter events within the plastic array. These are events (from ^{137}Cs) which scatter between the plastic elements and the central calorimeter. The spatial resolution of the PSPMT cleatly distinguishes individual 5mm plastic elements.

an approach has succeeded in resolving individual 3mm YAP crystal elements using a center-of-gravity calculation for determining the interaction location.[10] The utility of this readout scheme for rejecting multiple scatter events will be investigated. Given the mean free path of photons in plastic (6 cm at 100 keV), we expect that a high level of multiple scatter event rejection can be achieved with the fourteen channel readout scheme, thus minimizing the required number of electrical channels. If needed, we will more fully configure the PSPMT to test the multiple scatter event rejection at finer spatial scales.
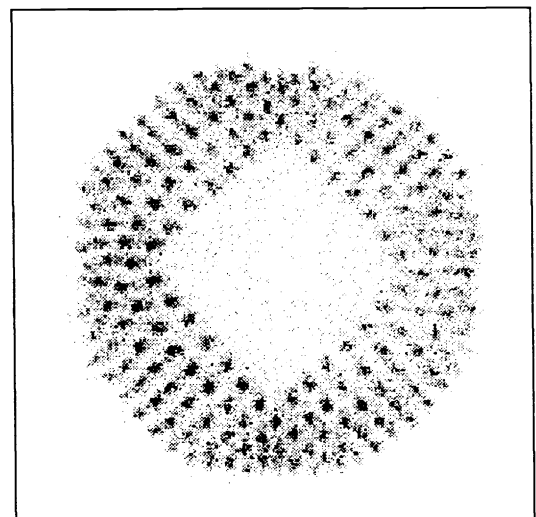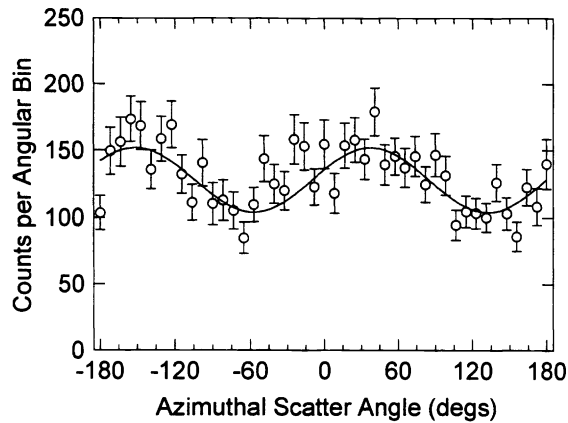
75

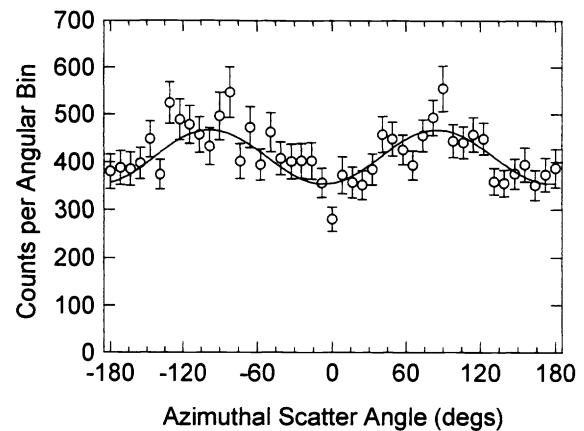Figure 10: The azimuthal scatter distribution for the baseline run with the SOLPOL science model.

Figure 11: The azimuthal scatter distribution for a run with the SOLPOL science model. In this case the plane of polarization was shifted by ~45° with respect to that in Figure 10.

Figure 9 shows the spatial distribution of Compton scatter locations within the plastic scintillator array. Unpolarized photons from a $^{137}$Cs source were used to directly illuminate the front surface of the polarimeter. Only events that were coincident between the plastic array and the central CsI(Tl) were recorded. The individual 5 mm plastic elements are clearly resolved by the PSPMT. These data suggest that even smaller elements could be used with this PSPMT. Also evident in the event distribution is the central well of the plastic array in which the calorimeter detector assembly is located.

Preliminary results of the science model response to a polarized laboratory beam have recently been obtained. These tests employed the use of a tagged polarized photon beam, as described in section 2. The analysis is limited in that the runs are of limited duration (poor event statistics), the spatial information within the calorimeter array is not yet utilized, and a proper energy calibration for each detector component is not yet available to optimize the event selection. A quantitative analysis of the polarimetric response is therefore not yet possible. Nonetheless, we have been able to demonstrate the existence of a polarization signal. This is seen in Figures 10 and 11, which show the azimuthal modulation of the scattered photon events at two different polarization angles offset by ~45°. In each case, the curve represents a fit to the data. The measured shift in the minimum of the modulation pattern, from about –60° in Figure 10 to about –10° in Figure 11 is consistent with the change in polarization angle of the incident beam (to within the accuracy of the experimental setup).

Further testing is currently underway to more completely characterize the performance of the science model. This will include a more complete analysis of several runs made at a variety of different energies, along with a more complete comparison with simulations of the laboratory setup.

## 5. HARD X-RAY POLARIMETRY OF SOLAR FLARES

The principle motivation for studying the polarization of hard X-rays from solar flares is that such data can provide important information regarding the the extent to which the accelerated electrons are beamed during the flaring process. This would have potentially important implications for any model of solar flare particle acceleration. Only with polarization measurements can we probe the extent of the electron beaming for individual flares. Previous attempts to measure X-ray polarization from solar flares have been limited to energies below ~30 keV and the available data generally provides conflicting results on the X-ray polarization of solar flares. SOLPOL is designed to operate at higher energies (above 50 keV), where the contaminating effects of thermal X-ray emission can be minimized.[11] (The contamination in this case results from the polarization of initially unpolarized photons as a result of backscattering from the photosphere.) Theoretical models predict a range of possible polarization levels for the hard X-ray emission. In general, polarization levels as high as 10-15% can be expected.[12]
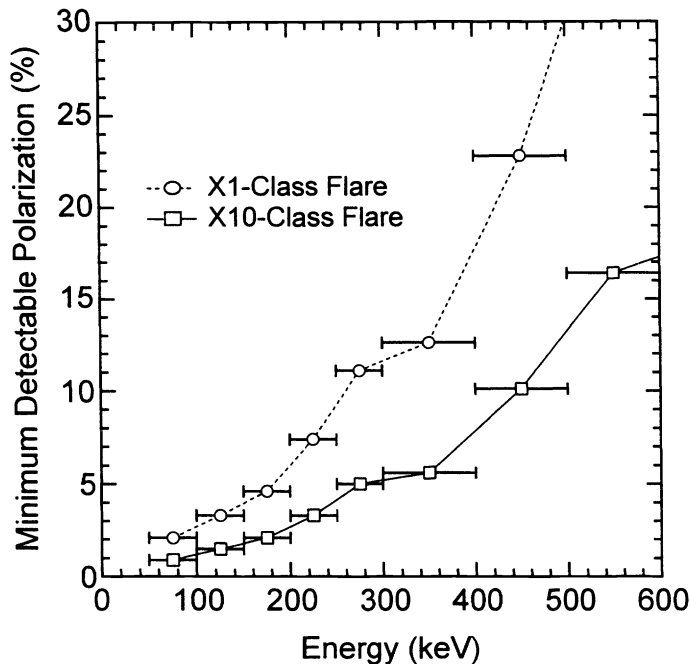
76

Figure 12: Estimates for the minimum detectable polarization (MDP) of a 16-element balloon-borne SOLPOL array in various energy bands for two different size solar flares.

In practice, the SOLPOL design would be used in the context of an array of polarimeter modules. Such an array could be made an integral part of either a long-duration balloon payload or an Earth-orbiting spacecraft payload. It is difficult to make specific predictions about the sensitivity of such an array to any one flare due to the unique nature of each individual flare event. We have, however, estimated the polarization sensitivity based on the SMM-measured spectrum for the flare of 7 June 1980. The assumed background is that of a balloon-borne payload. The resulting sensitivity estimates indicate that an array of sixteen modules would provide a minimum detectable polarization (MDP) of less than 1% in the integrated 50-300 keV energy range for some M-class flares and all X-class flares. Alternatively an array of four modules would provide a MDP of 1% or better in the integrated 50-300 keV energy range for all X-class flares. Figure 12 shows the MDP that is attained in smaller energy bands using a 16-element SOLPOL array for an X1- and an X10-class flare. MDP levels of a few percent should be sufficient to test various models for hard X-ray polarization in solar flares.

Another potential application for a SOLPOL-type module would be as a polarimeter that could be placed on the Particle Acceleration Solar Orbiter (PASO). PASO is a program currently being considered as a next-generation high energy solar observatory (part of the future roadmap for NASA's Sun-Earth Connection program). With a launch date of ~2012 (during solar maximum), it would be placed into a solar orbit at ~0.2 AU for observing high energy emissions from solar flares. At that distance, a single SOLPOL module would have the sensitivity equivalent to that of a 25-element SOLPOL array at 1 AU.

## 6. SUMMARY

The goal of the science model testing is to verify the performance characteristics of the SOLPOL design and to define the final electronics configuration. Once this has been accomplished, we can move forward with the detailed design and fabrication of a self-contained engineering model. We anticipate that this design would be used in the context of an array of polarimeter modules. An array of 16 modules would be capable of measuring solar flare polarization levels below 1% for the X-class flares and would also be capable of measuring polarization levels down to about 15% in some of the largest γ-ray bursts.[5] Although similar designs have been discussed in the literature,[11,13] we are unaware of any other active effort to develop specilaized hardware for measuring polarization in solar flares or in γ-ray bursts at energies above 100 keV.

In addition to its potential for studying transient sources, the SOLPOL design might also be useful in the context of an imaging polarimeter. For example, a SOLPOL element or array of elements could be used with a rotation modulation collimator to achieve arc-second angular resolution. Such an approach is not unlike that employed for hard X-ray imaging (without polarization capability) in the upcoming HESSI mission.[14] The spatial information intrinsic to the SOLPOL design might also be useful in a coded-aperture system, although perhaps limited to arc-minute angular resolutions.

## ACKOWLEDGEMENT

# REFERENCES

1. R.D. Evans, The Atomic Nucleus, New York: McGraw-Hill, 1958.
2. R. Novick, "Stellar and solar X-ray polarimetry," *Space Science Reviews*, vol. 18, pp. 389-408, 1975.
3. F. Lei, A.J. Dean and G.L. Hills, "Compton scatter polarimetry in gamma-ray astronomy," *Space Science Reviews*, vol. 82, pp. 309-388, 1997.
4. M. McConnell, D. Forrest, K. Levenson, and W.T. Vestrand, "The design of a gamma-ray burst polarimeter," in AIP Conf. Proc. 280, *Compton Gamma-Ray Observatory*, M. Friedlander, N. Gehrels and D.J. Macomb, Eds. New York: AIP, 1993, pp. 1142-1146.
5. M.L. McConnell, D.J. Forrest, J. Macri, J.M. Ryan, and W.T. Vestrand, "Development of a hard X-ray polarimeter for gamma-ray bursts," AIP Conf. Proc. 428, *Gamma-Ray Bursts*, C.A. Meegan and P. Cushman, Eds. New York: AIP, 1998, pp. 889-893.
6. M.L. McConnell, D.J. Forrest, J. Macri, M. McClish, M. Osgood, J.M. Ryan, W.T. Vestrand and C. Zanes "Development of a hard X-ray polarimeter for solar flares and gamma-ray bursts," *IEEE Trans. Nucl. Sci.*, vol. 45, no. 3, pp. 910-914, June, 1998.
7. H. Sakurai, M. Noma, and H. Niizeki, "A hard x-ray polarimeter utilizing Compton scattering," in *SPIE Conf. Proc.*, vol. 1343, pp.512-518, 1990.
8. W.H. McMaster, "Matrix representation of polarization," *Reviews of Mod. Phys.*, vol. 33, no. 1, pp. 8-28, January 1961.
9. M.L. McConnell, J.R. Macri, M. McClish, J. Ryan, D.J. Forrest and W.T. Vestrand, "Development of a Hrad X-Ray Polarimeter for Astrophysics," *IEEE Trans. Nucl. Sci*, in press, 1999.
10. R. Wojcik, S. Majewski, B. Kross, D. Steinbach, and A.G., "High spatial resolution gamma imaging detector based on a 5" diameter R3292 Hamamatsu PSPMT," *IEEE Trans. Nucl. Sci.*, vol. 45, no. 3, pp. 487-491, June, 1998.
11. G. Chanan, A.G. Emslie, and R. Novick, "Prospects for solar flare X-ray polarimetry," *Solar Physics*, vol. 118, pp. 309-319, 1988.
12. F. Lei, A.J. Dean, and G.L. Hills, "Compton polarimetry in gamma-ray astronomy," *Sp. Sci. Rev.*, vol. 82, pp. 309-388, 1997.
13. T.L. Cline, et al., "A gamma-ray burst polarimeter study," in *Proceedings of the 25th Internat. Cosmic Ray Conf.*, vol. 5, pp. 25-28, 1997.
14. .R. Dennis, et al., "The High Energy Solar Spectroscopic Imager – HESSI," in *SPIE Conf. Proc.*, vol. 2804, pp.228-240, 1996.